Phase equilibria of waxy live oil systems containing CO_2

Phase Equilibria of Waxy Live Oil Systems Containing CO_2: Experimental Measurements and Thermodynamic Modelling.

Oluwakemi V. Eniolorunda*, Antonin Chapoy, Rod Burgass.

Institute of GeoEnergy Engineering Heriot-Watt University, Riccarton Edinburgh, EH14 4AS. Edinburgh United Kingdom.

Ove2@hw.ac.uk*; A.Chapoy@hw.ac.uk, Rwb4@hw.ac.uk.

KEYWORDS: CO2, live oil, wax, WDT, Phase Equilibria, Thermodynamic modelling.

ABSTRACT: In this work, accurate experimental measurements of phase equilibrium data over a wide range of temperature and pressure were carried out for several synthetic live oil systems containing mixtures of hydrocarbons and CO2 employing an exponential decay in composition. The apparatus used in this study to measure the wax disappearance temperature (WDT) of the live oil systems consisted of a constant-volume visual cell rocking rig equipped with sapphire windows connected to a thermostatic bath with digital control. The data obtained were used to assess the predictive capability of existing phase equilibria thermodynamic models: The Peng-Robinson equation of state incorporating a group contribution method to calculate binary interaction parameters for fluid phase description and three different activity coefficient models for wax phase. Also, phase equilibria data gathered from the literature were modelled while comparing results from five high-pressure correction methods. The modelled results showed good predictability against the independent experimental data, demonstrating the robustness of the experimental procedure in this study.

Introduction

All components of crude oil are in thermodynamic equilibrium under reservoir conditions until production commences. The onset of production results in pressure changes that alters the phase equilibrium leading to phase transitions within the system. These pressure and temperature changes in the reservoir and pipelines could result in precipitation of solids such as wax, hydrate, asphaltene, and scale from the fluid phase. Waxes are solid hydrocarbon of relatively high molecular weight formed mainly due to a fall in temperature below the system solubility threshold. Several factors influence the precipitation, deposition, and/or growth of wax including crude oil composition, pressure, flow rate, pipe roughness and temperature. Waxy components of crude oil are not a problem until the temperature falls below the system's wax appearance temperature (WAT). WAT is the temperature at which heavy paraffin components of crude oil begin to precipitate followed by those of lower molecular weight turning the oil into a multi-phase mixture. The presence of this solid phase could result in increased viscosity, plugging of pipelines leading to increased power consumption, reduced production, reduction in ultimate recovery, and even worst-case scenario pipeline blockage with a potential loss of pipeline. WAT is a widely used parameter in the prediction of wax precipitation in the oil and gas industry unique to each crude oil type[1]. Experimental determination of WAT depends on measurement technique and factors such as heating and cooling rate of the oil, WAT obtained from different techniques can vary by up to 10K[2,3] for the same sample, hence, not satisfactory when validating thermodynamic models. Wax disappearance temperature (WDT): the temperature at which the last solid wax crystal is completely dissolved in the fluid phase is a point of thermodynamic equilibrium and hence a better parameter for describing wax phase boundary[4].

Many experimental procedures have been employed to obtain phase equilibria data especially for binary systems and a few of ternary and multicomponent systems by several researchers[5,6]. These procedures involved the use of: cross-polarization microscopy[7], viscometry[7], quartz crystal microbalance[8], differential scanning calorimetry[7], near-infrared spectroscopy[9], filter plugging[10], rheometry[11], light transmission[12] and visual observation[6,13,14,15].

In this study, a combination of visual observation and changes in system density due to wax formation and dissolution was employed for WDT measurements.

Thermodynamic modelling of phase behaviour of both synthetic and actual reservoir fluids in the presence of solid wax phase published in the literature assume iso-fugacity in all phases present[16]. Cubic EoS are widely used for VLE modelling, however,

calculating wax phase fugacity requires an activity model, for the sake of consistency, the liquid phase fugacity is calculated using the same cubic EoS for the VLE and SLE thermodynamic model for Solid-liquid-vapour equilibria (SLVE). There are several thermodynamic models reported in the literature for the solid (wax) phase descriptions based on different theories with varying degrees of precision.[16,6,17,18].

Description of liquid-vapour equilibria (VLE) and vapour-liquid-liquid equilibria (VLLE) is common in published articles. In contrast, SLE/SLVE is a rather rare topic of interest even though SLE/SLVE best describes wax problems. In this study, the influence of CO_2 on the SLE/SLVE of simple binary to multicomponent synthetic live oil systems were carried out checking the effect of composition and pressure on the phase transition of the systems. The next sections provide details of the experimental technique followed by a background of the SLE/SLVE modelling and then a review of CO_2 –hydrocarbon SLE/SLVE literature data and model predictions. The result and discussion section provides detailed comparison of the experimental data and modelled results gathered in this present work.

Experimental Section.

Test Fluids.

To measure the phase equilibrium of live oil systems, synthetic mixtures mimicking crude oil from the Brazilian pre-salt basin characterized by high gas-oil ratio (GOR) and CO_2 content is selected. Mixtures were prepared from commercially available chemicals. Each synthetic mixture was gravimetrically prepared with standard uncertainties of ± 0.01g for the hydrocarbons and ±0.015g for CO_2. The mixtures prepared in piston cylinders were kept monophasic by pressurizing the cylinder with injected Nitrogen gas behind the piston. To dissolve any solids present, erase history of solid formation and maintain a uniform temperature throughout the mixture, the prepared mixture is kept in an oven for 1hour at a temp well above the melting point of all systems considered (323.15K).

Table 1. Compositions of the synthetic mixtures (mole fractions).

Components	Sample 1	Sample 2	Sample 3	Sample 4	Sample 5	Sample 6	Sample 7
n- Dodecane($C_{12}H_{26}$)	0.128	0.205	0.293	0.378			
n-Hexadecane ($C_{16}H_{34}$)	0.093	0.149	0.212		0.860	0.560	0.160
n-Docosane ($C_{22}H_{46}$)	0.010	0.027	0.026	0.025			
n-Tricosane($C_{23}H_{48}$)	0.001	0.004	0.004	0.004			
n-Tetracosane($C_{24}H_{50}$)	0.007	0.018	0.019	0.017			
Carbon dioxide (CO_2)	0.761	0.597	0.446	0.576	0.140	0.440	0.840

Table 2 shows the chemical used, percentage purity and supplier. No further purification carried out.

Table 2. Fluids used in this study.

Fluids	%purity	source	CAS number
n-Hexadecane ($C_{16}H_{34}$)	99	Sigma-Aldrich	544-76-3
n- Dodecane($C_{12}H_{26}$)	99	Acros Organics	112-40-3
n-Docosane ($C_{22}H_{46}$)	99	Aldrich Chemicals	629-97-0
n-Tricosane($C_{23}H_{48}$)	99	Aldrich Chemicals	638-67-5
n-Tetracosane($C_{24}H_{50}$)	99	Aldrich Chemicals	117-18-
Carbon dioxide (CO_2)	99.995	BOC	124-38-9

Experimental equipment and procedures.

The equipment used in this study is an in-house designed visual rocking rig. The constant volume high-pressure rig comprised of a 100cc capacity steel cell with sapphire windows on both ends. To maintain equilibrium, 180° movement of the cell is achieved by mounting it on a pivot frame and movement controlled by a compressed air drive system operating at 6 cycles per minute. During experimental measurements made in this study the cell contents were continuously mixed, simulating production conditions.

The rig operates over a temperature range of 253.15-323.15K, and a maximum pressure of 51.7MPa. Automatic heating and cooling of the cell is achieved by circulating a coolant from a thermostatic bath through a jacket surrounding the cell. The temperature of

the sample in the cell is measured with a platinum thermometer calibrated against standard thermometer certified according to NAMAS accreditation standards and regulations. The temperature is measured within an accuracy of ±0.1K.

The pressure is measured with a Druck pressure transducer with an accuracy of ±0.04 MPa accuracy. The pressure transducer is regularly calibrated using a Budenberg deadweight tester.

The cell temperature and pressure are monitored and recorded through RS 232 outputs connected to the serial ports of a computer. Viewing of the cell contents is aided by means of a light source.

The WDT data were obtained from the visual rocking cell as shown in the scheme below by first maintaining the set up at a higher temperature than the expected WDT of the mixture using a Julabo thermostatic bath. The thermally equilibrated and monophasic mixture is then injected into the cell with a transfer line.

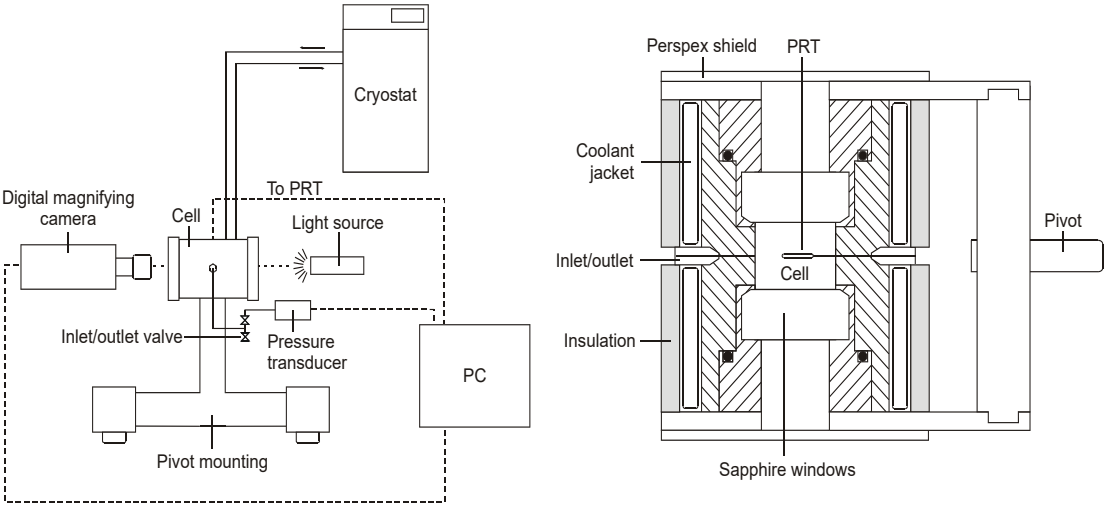

Figure 1 Schematic illustration of the wax Visual Rig experimental set-up and equilibrium cell (not to scale).

Once the desired volume of the mixture corresponding to the required pressure is transferred into the cell, the cylinder is disconnected, and the kinetic rig is set to rock at 10s interval using the pneumatic mixing system which allows for a well-mixed and homogenous system at all times. At constant pressure, the mixture temperature is decreased to 2K below the expected WDT over 2 hours and allowed to equilibrate for another hour.

The WDT is then measured by changing the temperature at 1°C steps and 0.5°C closer to the expected WDT and kept constant for 5 hoursmade possible by a programmable temperature profile of the Julabo bath which allows the mixture to equilibrate while heating the system stepwisely. Melting of the wax crystal is observed visually and the temperature at which the last wax crystal dissolves into the fluid phase is taken as the WDT of the system at that pressure. The visually observed WDT is further verified by a P-T plot of the lab view logged data as illustrated in Figure 2, the change in slope in the plot is an indication of a change in system density which corresponds to the WDT of the mixture at that pressure, both were consistently giving the same result. The use of graphical method for WDT measurement as a function of density change is however only applicable when vapour phase is present. This process is repeated for several pressure steps (Isobaric conditions) and for every mixture, the pressure is increased by injecting more mixture of the same composition into the cell.

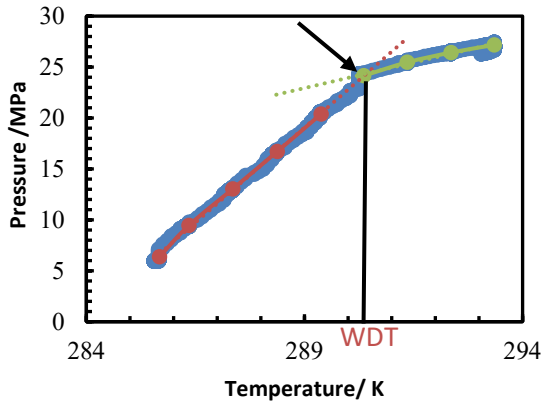

Figure 2. Sample P-T plot for determining mixture WDT by density change.

Thermodynamic modelling.

Accurate thermodynamic modelling of wax crystallization is important for good knowledge and appropriate description of wax formation processes which are vital steps towards overcoming wax problems. Phase equilibria models generally assumes equal temperature, pressure, and chemical potential in all phases present. Therefore, to model phases in thermodynamic equilibria, iso-fugacity criteria are usually adopted, this requires the fugacity; a more practical replacement for chemical potential of each phase to be calculated. For solid-fluid equilibria, the iso-fugacity approach is:

$$f_i^v = f_i^l = f_i^s \tag{1}$$

$$f_i^v = f_i^l = f_i^s \tag{2}$$

For a component i: $\boldsymbol{f_i^l}$ is the liquid phase fugacity, $\boldsymbol{f_i^v}$ the vapour phase fugacity and $\boldsymbol{f_i^s}$ solid phase fugacity:

Fluid phase model.

Depending on phases present, component fugacity can be calculated from either an appropriate equation of state or activity coefficient model. Due to the limited applicability of activity coefficient models to liquid and solid phases, fluid (liquid and vapour) phase fugacity is obtained from a cubic equation of state by expressing the fugacity as a function of the fugacity coefficients ϕ_i^v *and* ϕ_i^l:

$$f_i^v = x_i^v \phi_i^v P;\ f_i^l = x_i^l \phi_i^l P; \tag{3}$$

In this study, ϕ_i^v *and* ϕ_i^l are obtained from the Peng Robinson Equation of state (PR-EoS) due to it wide applicability and better prediction of similar systems as seen in published works. [19]

The pressure explicit form of the two-parameter PR EoS for a pure component is:

$$P = \frac{RT}{v-b} - \frac{a}{(v+b)(v-b)} \tag{4}$$

The classical mixing rule for calculating a and b is used to extend the EoS to mixtures.

$$a = \sum_{i=1}^{N}\sum_{j=1}^{N} z_i z_j \sqrt{a_i a_j}\left(1 - k_{ij}(T)\right); \qquad b = \sum_{i=1}^{N} z_i b_i \tag{5}$$

where k_{ij} is the binary interaction parameter (BIP) between components i and j and is calculated as a function of temperature, critical properties and acentric factor using the Mutlet and Jaubert group contribution approach (JMGC) [20]. This approach makes the EoS fully predictive as opposed to obtaining the k_{ij} from tuning experimental VLE data.

Solid-phase model.

There are a number of activity coefficient models based on different views of patterns followed during wax precipitation, this includes regular solution theory, ideal solution models, non-ideal solution models and multi-solid solution models[21,7]. The use of an appropriate activity coefficient model to describe the non-ideality of the solid phase will result in better-predicted wax phase transition. In this study, a comparison of the predictive capability of three (3) activity coefficient models for solid-liquid equilibria was conducted. The results of these models are compared with the experimentally measured solid-fluid phase boundary data. The

activity models studied includes, The original predictive UNIQUAC[22], modified Ji- UNIQUAC[23], and the Predictive Wilson model[24]. Description of the models are given in the next section.

At thermodynamic equilibrium:

$$f_i^l\left(P,T,x_i^l\right) = f_i^s(P,T,x_i^s) \tag{6}$$

The pure solid fugacity $\boldsymbol{f_i^{*s}}$, has been established to be related to that of the pure liquid phase, $\boldsymbol{f_i^{*l}}$, by:

$$\frac{f_i^{*l}}{f_i^{*s}} = exp\left(\frac{\Delta H_i^f}{RT}\left(1-\frac{T}{T_i^f}\right)+\frac{\Delta H_i^{tr}}{RT}\left(1-\frac{T}{T_i^{tr}}\right)\right) \tag{7}$$

This expression describes liquid to disordered solid and disordered solids to ordered solid phase transition.

The fugacity of components in the solid mixture is calculated from:

$$f_i^s = x_i^s\gamma_i^s f_i^{*s} \tag{8}$$

γ_i^s is calculated from the activity coefficient model described below.

UNIQUAC Model

This is a local compositional model developed by Abrams and Prausnitz (1975)[25]. The choice of the original form of this model is due to its wide applicability to asymmetric systems and fewer adjustable parameters making it of better accuracy. This model splits the activity coefficient to residual (R) and combinatorial (C) terms expressed as:

$$ln\,\gamma_i = ln\,\gamma_i^C + ln\,\gamma_i^R \tag{9}$$

$$\begin{aligned} ln(\gamma_i^c) &= ln\frac{\Phi_i}{x_i} \\ &+\frac{Z}{2}q_i\,ln\frac{\psi_i}{\Phi_i}+\left((r_i-q_i)\frac{Z}{2}-(r_i-1)\right) \\ &-\frac{\Phi_i}{x_i}\sum_j^{n_c}x_j\left(\left(r_j-q_j\right)\frac{Z}{2}-\left(r_j-1\right)\right) \end{aligned} \tag{10}$$

$$\mathrm{d}\ ln(\gamma_i^R) = q_i\left(1-ln\left(\sum_j^{nc}\psi_j\tau_{ji}\right)-\sum_j^{n_c}\left(\frac{\psi_j\tau_{ij}}{\sum_k^{n_c}\psi_k\tau_{kj}}\right)\right) \tag{11}$$

$$\psi_i = \frac{q_ix_i}{\sum_i^{n_c}q_ix_i};\Phi_i = \frac{r_ix_i}{\sum_i^{n_c}r_ix_i};\tau_{ji} = exp\left(-\frac{\lambda_{ji}-\lambda_{ij}}{q_iRT}\right) \tag{12}$$

$$r_i = 0.6744CN_i + 0.4534;\ q_i = 0.540CN_i + 0.616 \tag{13}$$

$\lambda_{ji} = \lambda_{ii}$, i is the component with the shorter chain length in the pair.

$$\lambda_{ii} = -\frac{2}{Z}\left(\Delta H_i^{sub} - RT\right) \tag{14}$$

$$\Delta H_i^{sub} = \Delta H_i^f + \Delta H_i^{tr} + \Delta H_i^{vap} \tag{15}$$

The thermo-physical properties for pure components of the mixture, $\Delta H_i^{tr}, T_i^{tr}, T_i^f,\ \Delta H_i^f$ for this model were obtained from the National institute of standards and technology (NIST) database.

Predictive Wilson Model.

This predictive local composition model describes the non-ideality of solid-phase by expressing γ_i^s as [24]:

$$ln\gamma_i^s = 1 - ln\sum_i x_j^s \Lambda_{ij} - \sum_k \frac{x_k^s \Lambda_{ki}}{\sum_j x_j^s \Lambda_{kj}} \quad (16)$$

$$\Lambda_{ij} = exp\left[-\frac{\lambda_{ij}-\lambda_{ii}}{RT}\right] \quad (17)$$

λ_{ii} is as described by equation (14).

Ji-UNIQUAC

Calculation of solid phase fugacity requires accurate fusion properties and heat capacities values. Ji et al [26] developed new correlations for these properties from experimental data of n-paraffins up to C_{70}. To model solid phase (wax), these correlations alongside selected critical properties calculation methods and the original UNIQUAC model were used. An investigation of this approach is to see if wax phase will be better predicted with the newly introduced correlations compared to the original UNIQUAC model. The introduced correlation for the carbon range covered in this study are presented below:

Paraffin with odd carbon numbers.

For $C_9<C_n\leq C_{43}$:

$$T_i^f = 0.0122C_n^2 - 2.0861C_n - \frac{775.598}{C_n} + 76.2189\, ln\, C_n + 156.9 \quad (18)$$

$$\Delta H_i^f = 0.74\Delta H^{sum};\ \Delta H_i^{tr} = 0.26\Delta H^{sum} \quad (19)$$

For $C_9<C_n\leq C_{33}$:

$$\Delta H_i^{sum} = 0.167mw \times T_i^f + 432.47 \quad (20)$$

For Paraffin with even carbon numbers and $C_{10}<C_n\leq C_{42}$:

$$T_i^f = 0.0031C_n^3 - 0.3458C_n^2 + 14.277C_n + 137.73 \quad (21)$$

$C_n\leq C_{20}$:

$$\Delta H_i^f = 1.0\Delta H^{sum}; \Delta H_i^{tr} = 0 \quad (22)$$

For $C_{20}<C_n\leq C_{42}$:

$$\Delta H_i^f = 0.64\Delta H^{sum}; \Delta H_i^{tr} = 0.36\Delta H^{sum} \quad (23)$$

$C_n\leq C_{34}$:

$$\Delta H_i^{sum} = 0.180mw \times T_i^f + 522.7 \quad (24)$$

Comparative Investigation for High-Pressure correction.

Accurate prediction of wax phase boundary depends on the combination of EOS, activity coefficient models, and thermophysical property correlations employed. With the right combination of the above, the predicted wax phase boundary should be in a close match with experimental data, especially at low pressure. At elevated pressures, the gap between the predicted and measured values becomes significantly wide. The following subsections describe and compare the performance of some high-pressure correction methods available in the literature. Some of these methods employed the Poynting correction approach: This approach introduces additional terms to the liquid to solid fugacity ratio expression thereby translating fugacity calculated at reference pressure to that the operating pressure (high pressure) while others use a no-Poynting method by basically adjusting the temperature and enthalpies of fusion and solid-solid transition for high pressure operations as described in the following subsections.

Pauly et al model(Pauly et al>, 2000).

For high-pressure correction, Pauly et al introduced a Poynting term, a function of the difference between wax forming paraffins liquid and solid molar volumes expressed as:

$$\frac{\beta}{RT}\int_{P_o}^{P} v_i^l dP = \beta\, ln\frac{f_i^{*l}(P)}{f_i^{*l}(P_0)} \tag{25}$$

β, a pressure independent parameter for converting molar volume of pure component to that of components in solid solutions.

Equation(7) upon addition of the high-pressure term becomes:

$$\frac{f_i^{*l}}{f_i^{*s}} = exp\left(\frac{\Delta H_i^f}{RT}\left(1-\frac{T}{T_i^f}\right)+\frac{\Delta H_i^{tr}}{RT}\left(1-\frac{T}{T_i^{tr}}\right)\right)+\frac{\beta}{RT}\int_{p_0}^{p}\left(v_i^l\right)dp \tag{26}$$

Modified Ji Approach

The model based on solid solution theory uses the Poynting term approach. Different from other Poynting methods, the added term to the fugacity ratio expression is a pressure dependent term considering the difference between reference and operating pressures as shown in equations(27) and (28).

$$\frac{f_i^{*l}}{f_i^{*s}} = exp\left(\frac{\Delta H_i^f}{RT}\left(1-\frac{T}{T_i^f}\right)+\frac{\Delta H_i^{tr}}{RT}\left(1-\frac{T}{T_i^{tr}}\right)\right)+\frac{1}{RT}\int_{p_0}^{p}(v_i^s)dp \tag{27}$$

$$\frac{1}{RT}\int_{p_0}^{p}(v_i^s)dp = \frac{P-P_0}{RT^2}\left(\frac{\Delta H_i^f}{\left(dP^{sat}/_{dT}\right)^f}+\frac{\Delta H_i^{tr}}{\left(dP^{sat}/_{dT}\right)^{tr}}\right) \tag{28}$$

Ghanaei et al Model[28]

The multi-solid approach of Ghanaei et al [28] for fugacity ratio calculations at high pressures is based on the Clapeyron equation as shown in equations (29) and (30). The authors used this equation coupled with various version of the UNIQUAC model to predict the non-ideality in the solid wax phase, however in this work; only the original predictive UNIQUAC model was checked.

$$\frac{f_i^{*l}}{f_i^{*s}} = exp\left(\frac{\Delta H_i^f}{RT}\left(1-\frac{T}{T_i^f}\right)+\frac{\Delta H_i^{tr}}{RT}\left(1-\frac{T}{T_i^{tr}}\right)\right)+\frac{1}{RT}\int_{p_0}^{p}\left(v_i^l-v_i^{os}\right)dp \tag{29}$$

The second term in Equation(29) is the high-pressure Poynting term relating the liquid molar volume $\boldsymbol{v_i^l}$ to the ordered solid molar volume $\boldsymbol{v_i^{os}}$:

$$v^l - v^{os} = \frac{\Delta H^f}{T\left(dp^{sat}/_{dT}\right)^f}+\frac{\Delta H^{tr}}{T+\left(dP^{sat}/_{dT}\right)^{tr}} \tag{30}$$

Mahabadian et al model[29]

This model followed the no-Poynting correction approach. Instead of adding a pressure correction term to existing fugacity ratio expression, Mahabadian et al[29] considered the pressure dependency of temperature, enthalpies of fusion and solid-solid

transition by modifying their values at a reference pressure to account for high pressure effect. The thermophysical properties at reference pressure P_o are from NIST database.

At high pressure:

$$H_i^f(P) = (v_i^L(P) - v_i^S(P))T_i^f(P)\left[\frac{dP^{sat}}{dT_f}\right]_i;\ \Delta H_i^{tr}(P) = 1 - \beta(P)T_i^{tr}(P)\left[\frac{dP^{sat}}{dT_{tr}}\right]_i \tag{31}$$

$$v_i^S = \beta v_i^L \tag{32}$$

$$\beta(P) = \beta(P_0) + \alpha(P - P_0) \tag{33}$$

β is a pressure dependent term and α is an adjustable parameter dependant on the mixture, it value for the binary mixtures considered by the author are reported in the article[24].

$$T_i^{tr}(P) = T_i^{tr}(P_0) + \left(\frac{P - P_0}{\left(dP^{sat}/dT_{tr}\right)}\right);\ T_i^f(P) = T_i^f(P_0) + \left(\frac{P - P_0}{\left(dP^{sat}/dT_f\right)}\right) \tag{34}$$

$$dP^{sat}/dT_f = 4.5;\ \ dP^{sat}/dT_{tr} = 3.5 \tag{35}$$

Nasrifar and Fani Khesty Model[30].

This model is based on the description of the solid-liquid coexistence curve by a form of the Clapeyron equation and the assumption that paraffin wax mixtures are orthorhombic with disordered solid to ordered solid transition occurring before melting.

Equations (36) and (37) are the high-pressure expressions adopted by the authors.

$$T\left(v_i^l - v_i^s\right) = \partial\left(\frac{\Delta H_i^f + \Delta H_i^{tr}}{R}\right) \tag{36}$$

$\delta = 0.002 m^3/Kmol$ for C_8-C_{40} paraffin waxes.

Equation (7) becomes:

$$\frac{f_i^{*l}}{f_i^{*s}} = exp\left(-\partial\left(\frac{\Delta H_i^f + \Delta H_i^{tr}}{R^2 + T^2}\right)(P - P_0) - \frac{\Delta H_i^f}{RT}\left(1 - \frac{T}{T_i^f}\right) - \frac{\Delta H_i^{tr}}{RT}\left(1 - \frac{T}{T_i^{tr}}\right)\right) \tag{37}$$

Literature review

Phase Equilibria

The ability of thermodynamic models to predict the phase behaviour of crude oil systems is fundamental for proper process design[20]. Accuracy of these models depends on the availability of experimental data with which they can be tuned and adjusted. Depending on the crude oil composition and operating conditions, model predictability varies. CO_2 is a major non-hydrocarbon component of crude oil and the increasing interest of the petroleum industry in CO_2 enhanced oil recovery has further necessitated the study of CO_2-hydrocarbon systems. The majority of phase equilibrium studies of CO_2+n-alkanes reported in the literature are vapour-liquid equilibria (VLE)[16,3132,33,6, 14, 34, 35,36,37,5,38] and liquid-liquid equilibria (LLE)[5,39] with limited work on solid-liquid equilibria (SLE)[6,15,14, 40] especially for multicomponent systems of heavy alkanes.

In this section, a review of published solid-fluid phase transition data is carried out on binary and multicomponent systems containing CO_2 and heavy n-alkanes. A total of 122 data for both SLE and SLVE (Solid liquid vapour equilibria) were gathered from literature, 79 of those were measurements made on binary mixtures of CO_2 and n-alkanes including hexadecane, eicosane, docosane and triacontane [14, 15,4115] and the other 43 were for multicomponent mixtures of CO_2, dodecane, docosane, tricosane and tetracosane over a range of pressure and CO_2 mole fraction distribution as shown in Table 3. These data gathered from the

literature were mostly by visual observation of solid appearance at a given pressure and the corresponding temperature taken as the WAT.[14,6] [15] except for data from Reverchon et al [41] which used flow type apparatus.

Table 3. Published data for solid-fluid equilibria for mixtures of carbon dioxide- n-alkane systems.

Mixture	No of data points	Pressure (MPa)		CO_2 mole fraction		Equilibrium conditions	Best fit Activity coefficient model	Statistical analysis of modelled vs experimental temperature		Reference
		Min	Max	Min	Max			ASTD	AAPE (%)	
$CO_2/C_{16}H_{34}$	14	15.7	141.9	0.98	0.99	SLE	Ji-UNIQUAC	1.78	1.06	[42]
$CO_2/C_{16}H_{34}$	12	27.6	146.3	0.32	0.64	SLE	Original UNIQUAC	1.06	0.51	[42]
$CO_2/C_{22}H_{46}$	11	1.0	6.9	0.13	0.65	SLVE	Ji-UNIQUAC	1.05	0.48	[14]
$CO_2/C_{20}H_{42}$	5	7.1	25.0	0.98	0.98	SLLE	Original UNIQUAC	0.79	0.37	[15]
$CO_2/C_{20}H_{42}$	6	8.1	14.1	0.99	0.99	SLE	Original UNIQUAC	3.67	1.73	[15]
$CO_2/C_{20}H_{42}$	13	0.5	6.6	0.30	0.93	SLE	Original UNIQUAC	1.01	0.47	[15]
$CO_2/C_{30}H_{62}$	9	10.5	25.0	0.99	0.99	SVE	Original UNIQUAC	7.53	3.35	[41]
$CO_2/C_{30}H_{62}$	9	9.0	25.0	0.99	0.99	SVE	Original UNIQUAC	7.17	3.29	[41]
$CO_2/C_{12}H_{26}/C_{22}H_{46}$ $/C_{23}H_{48}/C_{24}H_{50}$	13	2.1	59.97	0.20	0.40	SLE	Original UNIQUAC	0.48	0.58	[6]
$CO_2/C_{12}H_{26}/C_{22}H_{46}$ $/C_{23}H_{48}/C_{24}H_{50}$	13	4.7	69.9	0.40	0.80	SLE	Ji-UNIQUAC	0.77	0.37	[6]
$CO_2/C_{12}H_{26}/C_{22}H_{46}$ $/C_{23}H_{48}/C_{24}H_{50}$	8	0.2	3.4	0.20	0.40	SLVE	Original UNIQUAC	1.01	0.47	[6]
$CO_2/C_{12}H_{26}/C_{22}H_{46}$ $/C_{23}H_{48}/C_{24}H_{50}$	9	0.2	5.1	0.40	0.80	SLVE	Ji-UNIQUAC	0.87	0.42	[6]

The gathered experimental data were used to check the predictive capability of PR-EoS and the activity coefficient models listed earlier. Statistical analysis of the measured WATs versus model prediction is represented by the average absolute percentage error (AAPE) and average standard deviation (ASTD) as shown in Table 3. For the binary mixtures, Predictive Wilson and Original UNIQUAC activity coefficient models gave the same prediction, reason being that the major variables (BIPs, and thermos-physical properties) were obtained by the same approach in both cases, thermophysical properties were from NIST database and BIPs through the group contribution approach. Ji-UNIQUAC approach predicted a different result from the other two as the authors correlation for determining thermophysical was used in place of those from database. **Table 3** above summarizes the reviewed data as well as the statistical analysis of best performing models, original UNIQUAC model was reported for binary systems. Common to all, systems with lower CO_2 were better correlated with lower deviation. This behaviour is consistent with data gathered from measurement made in this current study as shown in **Figure 3**. However, mixture of $CO_2/C_{30}H_{62}$ gave the highest AAPE of 3.35% which is not surprising as the data were very limited, and a different measurement technique was used.

Predicted data by original UNIQUAC and Ji- UNIQUAC activity coefficient model best described the multicomponent systems containing 0.2, 0.4mol% CO_2 and 0.6 and 0.8mol% CO_2, respectively.

It is very important to mention that the transition temperature measured for these systems from literature were those of fluid to solid transition (WAT). As earlier mentioned in this article, WAT does not represent a state of true thermodynamic equilibrium hence the discrepancy observed between the measured experimental data and the model prediction of WDT for such systems.

Results and Discussion.

Solid-fluid equilibria of binary mixtures of CO_2+n-hexadecane and multicomponent mixtures containing CO_2 +n-hexadecane+dodecane+docosane+tricosane+tetracosane were investigated for pressures up to 24MPa. The WDT of the systems were measured at pressures below and above bubble point i.e., both SLVE and SLE were studied.

To investigate the effect of CO_2 on the phase behaviour of binary and multicomponent systems, measurements were carried out on several samples with various CO_2 composition. **Table 1** shows the composition of the 7 mixtures while the measured WDT alongside the standard deviation error bar over three different trials and observed phase transitions at everypressures are presented in **Table 4**.

Table 4. Experimental phase equilibrium data for Investigated mixtures

T/K	P/MPa	Phases	T/K	P/MPa	Phases
Sample 1					
284.3±0.3	3.32	L+V+S→L+V	286.7±0.5	17.81	L+S→L
283.3±0.2	4.38	L+V+S→L+V	287.1±0.9	18.92	L+S→L
284.4±0.6	9.14	L+S→L			
Sample 2					
292.3±0.4	2.05	L+V+S→L+V	289.9±0.6	4.51	L+V+S→L+V
289.8±0.4	3.54	L+V+S→L+V	290.9±1.6	16.06	L+S→L
288.8±0.7	4.21	L+V+S→L+V	291.7±1.6	18.42	L+S→L
Sample 3					
289.7±0.7	1.83	L+V+S→L+V	288.2±0.9	5.20	L+S→L
287.7±0.2	2.69	L+V+S→L+V	289.2±1.2	10.48	L+S→L
287.7±0.4	3.37	L+S→L	290.2±1.0	15.95	L+S→L
Sample 4					
290.5±0.2	1.68	L+V+S→L+V	287.8±0.6	8.27	L+S→L
287.8±0.3	3.23	L+V+S→L+V	290.7±1.4	20.11	L+S→L
287.5±0.6	4.16	L+V+S→L+V			
Sample 5					
290.0±0.6	0.87	L+V+S→L+V	290.3±0.7	11.81	L+S→L
289.1±0.20	1.57	L+V+S→L+V	291.3±0.8	14.99	L+S→L
290.0±0.3	7.65	L+S→L	291.6±0.5	15.40	L+S→L
Sample 6					
289.4±0.4	1.03	L+V+S→L+V	285.8±0.8	5.01	L+S→L
288.3±0.2	1.68	L+V+S→L+V	289.4±0.6	20.28	L+S→L
287.4±0.4	2.19	L+V+S→L+V	290.4±0.7	24.40	L+S→L
Sample 7					
289.6±0.1	1.54	L+V+S→L+V	284.4±0.3	3.79	L+V+S→L+V
287.4, ±0.5	2.54	L+V+S→L+V	279.2±0.3	4.13	L+V+S→L+V
285.3±0.3	3.50	L+V+S→L+V	279.7±0.4	9.14	L+S→L

Binary systems of CO_2 and $C_{16}H_{34}$.

Due to complexities associated with measurement and prediction of wax formation in crude oil systems, accurate measurement of thermodynamic solid-fluid transition temperature can be done by establishing a reliable measurement approach for simple two-component fluids.

WDTs of three binary mixtures of CO_2 +n-hexadecane containing 84, 44 and 14 mol% CO_2 respectively were measured using the approach and equipment described earlier in the experimental equipment and procedure section. Sample 5-7 in **Table 4** shows

the results of the measurements. The wax disappearance temperature (WDT) at different pressures were obtained by visual observation which was verified with logs of the pressure-temperature data from stepwise heating with a change in density causing a change in slope indicating WDT for regions with vapour phase, with both approaches giving the same result. The use of computer programming to log temperature and pressure data allowed real time measurement to be made. The combined WDT data and corresponding pressure for each mixture allowed the P-T phase boundary line to be plotted as shown in **Figure 3**.

It can be observed that increasing CO_2 content of the mixtures reduces it WDT. This result is consistent with the findings from the literature review as well as those from a previously published article[43]. This also proves the ability of CO_2 as a light end gas to extract heavier components from oil systems making it a flow improver with the chance of keeping the system WDT below the surrounding temperature.

Thermodynamic modelling of the binary mixtures as shown by the lines in **Figure 3** were carried out using a combination of PR-EoS with classical mixing rules, the JMGC approach for BIPs to overcome the challenges posed by the sensitivity of BIPs to CO_2-hydrocarbon mixtures when it is tuned with VLE data, and the original predictive UNIQUAC model gave the best description out of all three activity models.

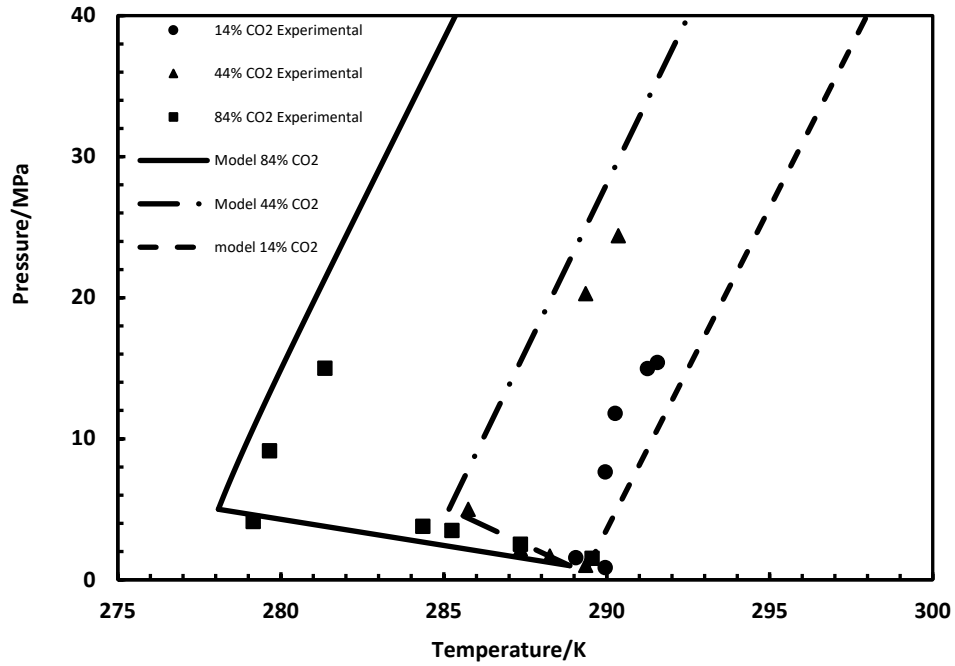

Figure 3. Experimental and model Solid-fluid phase equilibria data of 3 binary mixtures of CO_2 and n-$C_{16}H_{34}$.

The predictive Wilson and original UNIQUAC model yielded the same result with 0.5%AAPE while Ji-UNIQUAC predicted the data with 0.7%AAPE. These well-predicted results further validate the reliability of the experimental equipment and procedure. This encouraged the use of the same experimental technique to obtain phase equilibrium data for more complex mixtures similar to real crude oil systems.

Multicomponent systems containing CO2+n-alkanes

New phase equilibria measurements of mixtures of CO_2, n-$C_{12}H_{26}$, n-$C_{16}H_{34}$, n-$C_{22}H_{46}$, n-$C_{23}H_{48}$ and n-$C_{24}H_{50}$ for 44.6, 57.6, 59.7 and 76mol% CO_2 at pressures up to 20MPa were carried out. In this work, measurements were focused on obtaining the actual thermodynamic solid phase transition temperature (WDT) and to also study the impact of varying carbon dioxide composition on systems phase equilibria. Results are presented in Table 4.

Measurements were made both in regions of saturation and under saturations. The WDT generally increased with increasing pressure up to the saturation point after which it starts to decrease. The intersection between two phase and single phase WDTs corresponds to the system's bubble point. As expected, the WDT decreases with increasing CO_2 concentration.

Figure 4. Shows a how the experimentally measured solid wax phase boundary data in this work compares with predictions from activity models, including the original predictive UNIQUAC, Ji-UNIQUAC, predictive Wilson activity coefficient models and

a high pressure correction approach according to Pauly et al [27]. The fluid phases being described by Peng Robinson equation of state with JMGC for BIP and the classical mixing rule.

For all multicomponent systems studied, the original predictive UNIQUAC model described the mixture phase equilibria best with an AAPE of 0.27% except for sample 2 containing 59.7mol%CO_2 being slightly better described by the Ji et al modification of

the UNIQUAC model. The difference between prediction by the original UNIQUAC and Ji-UNIQUAC is by an average of 0.004. All activity coefficient models showed a positive deviation from the experimental data.

Similar to common reports in published articles, all three activity models showed greater deviations from measured value at high pressures. Applying the Poynting approach of Pauly et al coupled with original UNIQUAC model, we saw a slight improvement in the results predicted with a new AAPE of 0.26%.

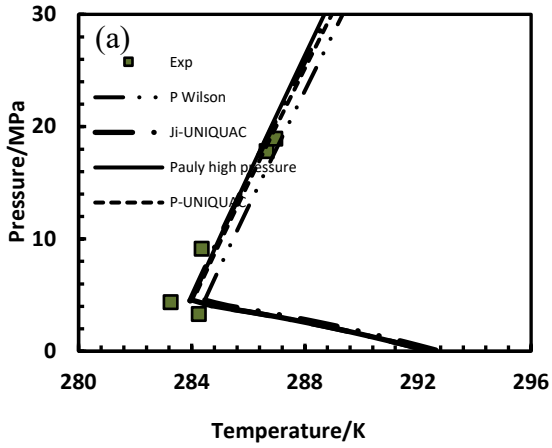

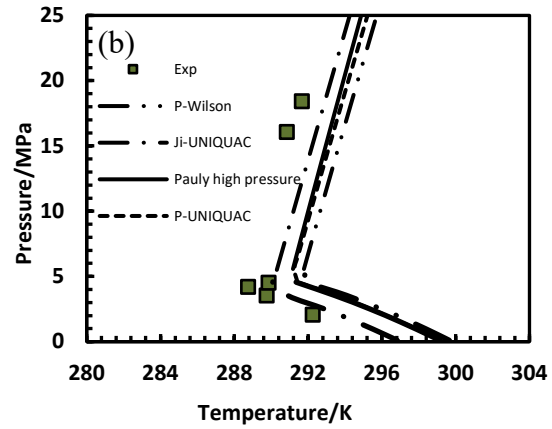

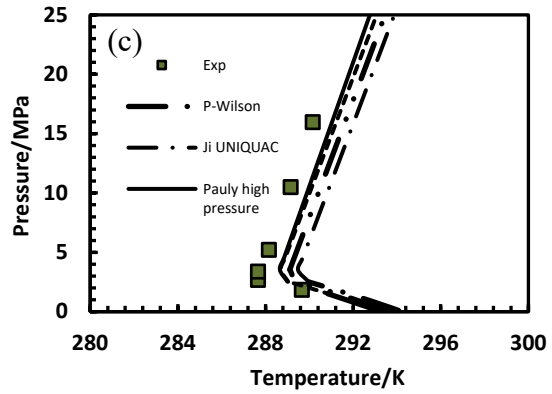

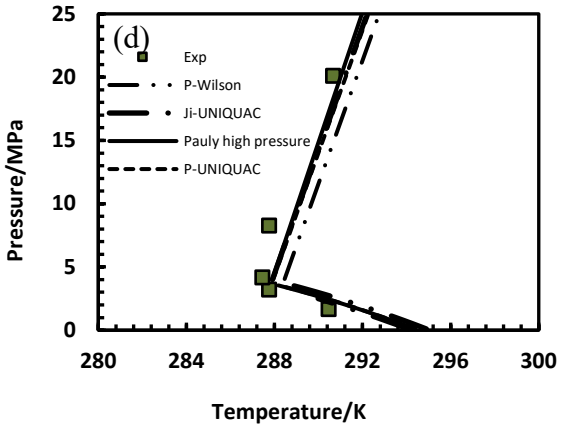

Figure 4. Experimental and calculated solid-fluid phase boundary for multicomponent systems using different activity coefficient models. a) Sample 1 (76.1% CO_2) b) sample 2 (59.7% CO_2) c) sample 3 (44.6% CO_2) d) Sample 4 (57.6% CO_2).

High-pressure Correction methods

For the range of pressures (0.87-24MPa) considered in this work, a high-pressure Poynting term approach slightly improved the performance of the solid phase models.

A comparison of the impact of high pressure correction methods on fugacity ratio calculations was done using 43 multicomponent CO_2 +n-alkanes (dodecane, docosane, tricosane and tetracosane) solid fluid equilibria data reported in an article published by da Silva et al [6]. The published results included both regions of SLVE and SLE, for the purpose of the high-pressure correction investigation, only the liquid to solid phase equilibria (SLE) data were used. The data spread across 4 samples containing 20, 40, 60 and 80mol% CO_2, respectively. The no Poynting high pressure method presented by Mahabadian et al[29] for highly asymmetric systems gave the best prediction for samples 1 and 2 with an average deviation of 0.7,and 0.4 respectively. As the CO_2 concentration increased, the accuracy of the models changed, samples 4 and 5 containing 60 and 80mol% CO_2 were best fitted by the pressure independent Poynting method of Pauly et al[27] with 0.05 and 0.76 deviations respectively from experimental values.

As more CO_2 + n-alkanes multicomponent data becomes available the reliability of the high-pressure correction methods mostly developed for systems containing methane rather than CO_2 can be further evaluated and if necessary, a new one developed for CO_2 rich systems.

Conclusions

In this work, experimental phase equilibrium data for seven synthetic mixtures (three binary and four multicomponent) comprising of CO_2, n-$C_{12}H_{26}$, n-$C_{16}H_{34}$, n-$C_{22}H_{46}$, n-$C_{23}H_{48}$ and n-$C_{24}H_{50}$ were obtained by measuring the thermodynamic wax disappearance temperatures (WDT) using a new approach of combining visual inspection and system density change. Regions of both SLE and SLVE were observed and gathered data are reported. The measured data for all samples showed the wax phase boundary.

For all systems studied, increasing the CO_2 content resulted in a reduced WDT, an indication of the ability of CO_2 as a light end gas to improve flow and allow transportation in cooler temperatures with a lower risk of wax precipitation.

A detailed literature review showing the capability of three activity coefficient model for solid phase description was carried out while predicting the fluid phase with the popular PR EoS using data gathered from published articles. It can be concluded that:

For CO_2+n-alkane binary mixtures, most of the data were better predicted by both predictive Wilson and original UNIQUAC models which yielded the same result as expected since the thermophysical properties and binary interaction parameters were calculated using the same approach. Ji-UNIQUAC best predicted results for binary mixtures of CO_2+ n-$C_{16}H_{34}$ with 99.999mol% CO_2. The largest deviation was seen in mixtures containing triacontane which could be due to the measurement technique and the availability of very few data.

Extending the model study to multicomponent CO_2+n-alkane (dodecane, docosane, tricosane and tetracosane) mixtures, for both SLVE and SLE, Ji-UNIQUAC activity coefficient model gave the best description for systems with high CO_2 concentration while Original UNIQUAC model best described systems with lower CO_2 content.

The ability of these thermodynamic models to successfully describe literature binary and multicomponent systems encouraged the application to studied mixtures. It was observed for binary systems of CO_2 +n-hexadecane, increasing the CO_2 concentration resulted in a considerable higher deviation of modelled result from experimental values. It was seen that mixture containing 14mol% CO_2 deviated by 0.48 from the measured data while that containing 84mol% CO_2 had an average deviation of 1.3 and those of 44mol% CO_2 lies between with deviation higher than those of 84mol% CO_2.

Similar to the binary systems, the prediction of the multicomponent experimental phase boundary data by the thermodynamic models yielded better results for systems with 44.6mol% CO_2 than those with 76% CO_2 while the model accuracy for sample 2 with

59.7% CO_2 lie in between for all activity models with the original predictive UNIQUAC giving the best description for samples 1,3 and 5 while modification of the original UNIQUAC model by Ji et al (Ji-UNIQUAC) best described sample 2.

In addition, the Pauly et al Poynting high pressure method alongside the original UNIQUAC model yielded a very small improvement of just 0.0085%AAPE over the original UNIQUAC model with no high-pressure correction.

For the comparative study of high-pressure correction methods carried out using multicomponent CO_2+n-alkane SLE data gathered from literature, the no Poynting approach presented by Mahabadian et al[29] for highly asymmetric systems gave the best prediction for samples 1 and 2 containing 60 and 80 mol%CO_2 with an average standard deviation of 0.7, 0.33% AAPE for sample 1 and ASTD of 0.4 and 0.21% AAPE for sample 2. However, with increased CO_2 concentration the accuracy of the models changed and for samples 4 and 5 containing 60 and 80 mol% CO_2 the pressure independent Poynting method of Pauly et al [44] with average deviation of 0.05 and 0.76 respectively gave a better description.

More experimental data might be needed to further validate the high-pressure methods.

ASSOCIATED CONTENT

List of symbols

f	fugacity
y	Vapour phase mole fraction
x	Liquid phase mole fraction
ϕ	Fugacity coefficient
P	Pressure
T	Temperature
υ	Molar volume
R	Universal gas constant
γ	Activity coefficient
λ	Interaction energy
H	Molar enthalpy
r, q	Structural parameters
Z	Lattice coordination number
ψ	Area component
Φ	Fractional volume component
Cn	Number of carbon atoms
MW	Molecular weight
Λ	Interaction parameter
B	Phase Fraction
δ	Phase boundary constant

Superscripts

l	Liquid phase
s	Solid phase
tr	Transition
f	Fusion
*	Pure
sub	Sublimation
vap	Vaporization
C	Combinatorial
R	Residual
sat	Saturation

subscripts

i,j	Component Index
o	reference

AUTHOR INFORMATION

Corresponding Author

Oluwakemi V. Eniolorunda. Institute of GeoEnergy Engineering Heriot-Watt University, Riccarton, EH14 4AS. Edinburgh, United Kingdom.

Ove2@hw.ac.uk;

Author Contributions

Oluwakemi V. Eniolorunda: Experimental data, calculations, modelling and writing.

Antonin Chapoy: Conceptualization, supervision, modelling and writing.

Rod Burgass: Experimental data and writing.

Notes

The authors declare no competing financial interests.

ACKNOWLEDGMENT

The authors acknowledge the financial support of the Petroleum Technology Development Fund (PTDF) Nigeria.

REFERENCES

1. Tiwary, D. & Mehrotra, A. K. Phase Transformation and Rheological Behaviour of Highly Paraffinic "Waxy" Mixtures. *Can. J. Chem. Eng.* **82**, 162–174 (2008).
2. Pedersen, W. B., Hansen, A. B., Larsen, E., Nielsen, A. B. & Rønningsen, H. P. Wax Precipitation from North Sea Crude Oils. 2. Solid-Phase Content as Function of Temperature Determined by Pulsed NMR. *Energy and Fuels* **5**, 908–913 (1991).
3. Roenningsen, H. P., Bjoerndal, B., Baltzer Hansen, A. & Batsberg Pedersen, W. Wax precipitation from North Sea crude oils: 1. Crystallization and dissolution temperatures, and Newtonian and non-Newtonian flow properties. *Energy & Fuels* **5**, 895–908 (2005).
4. Venkatesan, R., Singh, P. & Fogler, H. S. Delineating the pour point and gelation temperature of waxy crude oils. *SPE J.* **7**, 349–352 (2002).
5. Nieuwoudt, I. & Du Rand, M. Measurement of phase equilibria of supercritical carbon dioxide and paraffins. *J. Supercrit. Fluids* **22**, 185–199 (2002).
6. da Silva, V. M. *et al.* High pressure phase equilibria of carbon dioxide + n-alkanes mixtures: Experimental data and modeling. *Fluid Phase Equilib.* **463**, 114–120 (2018).
7. Ronningsen, H. P., Bjorndal, B., Hansen, A. B. & Pedersen, W. B. Wax Precipitation from North Sea Crude Oils. 1. Crystallization and Dissolution Temperatures, and Newtonian and Non-Newtonian Flow Properties. *Energy and Fuels* **5**, 895–908 (1991).
8. Létoffé, J. M., Claudy, P., Kok, M. V., Garcin, M. & Volle, J. L. Crude oils: characterization of waxes precipitated on cooling by d.s.c. and thermomicroscopy. *Fuel* **74**, 810–817 (1995).
9. Paso, K., Kallevik, H. & Sjöblom, J. Measurement of wax appearance temperature using near-infrared (NIR) scattering. *Energy and Fuels* **23**, 4988–4994 (2009).
10. Coutinho, J. A. P. & Daridon, J. L. The limitations of the cloud point measurement techniques and the influence of the oil composition on its detection. *Pet. Sci. Technol.* **23**, 1113–1128 (2005).
11. Ghannam, M. T., Hasan, S. W., Abu-Jdayil, B. & Esmail, N. Rheological properties of heavy & light crude oil mixtures for improving flowability. *J. Pet. Sci. Eng.* **81**, 122–128 (2012).
12. Uba, E., Ikeji, K. & Onyekonwu, M. Spe 88963. 1–9 (2004).
13. Sanchez-Vicente, Y., Tay, W. J., Al Ghafri, S. Z. & Trusler, J. P. M. Thermodynamics of carbon dioxide-hydrocarbon systems. *Appl. Energy* **220**, 629–642 (2018).
14. Fall, D. J. & Luks, K. D. Phase Equilibria Behavior of the Systems Carbon Dioxide + n-Dotriacontane and Carbon Dioxide + n-Docosane. *J. Chem. Eng. Data* **29**, 413–417 (1984).
15. Rodriguez-Reartes, S. B. *et al.* High-pressure phase equilibria of systems carbon dioxide + n-eicosane and propane + n-eicosane. *J. Supercrit. Fluids* **50**, 193–202 (2009).
16. Al Ghafri, S. Z., Maitland, G. C. & Trusler, J. P. M. Experimental and modeling study of the phase behavior of synthetic crude oil+CO_2. *Fluid Phase Equilib.* **365**, 20–40 (2014).
17. Pedersen, K. S. and Amount of Wax Precipitation. (1995).
18. Hansen, J. H., Fredenslund, A., Pedersen, K. S. & Rønningsen, H. P. A thermodynamic model for predicting wax formation in crude oils. *AIChE J.* **34**, 1937–1942 (1988).
19. Lopez-Echeverry, J. S., Reif-Acherman, S. & Araujo-Lopez, E. Peng-Robinson equation of state: 40 years through cubics. *Fluid Phase Equilib.* **447**, 39–71 (2017).
20. Jaubert, J. N. & Mutelet, F. VLE predictions with the Peng-Robinson equation of state and temperature dependent kij calculated through a group contribution method. *Fluid Phase Equilib.* **224**, 285–304 (2004).
21. Lira-Galeana, C., Firoozabadi, A. & Prausnitz, J. M. Thermodynamics of Wax Precipitation in Petroleum Mixtures. *AIChE J.* **42**, 239–248 (1996).
22. Coutinho, J. A. P. & Daridon, J. L. Low-pressure modeling of wax formation in crude oils. *Energy and Fuels* **15**, 1454–1460 (2001).
23. Ji, H. Y., Tohidi, B., Danesh, A. & Todd, A. C. Wax phase equilibria: Developing a thermodynamic model using a systematic approach. *Fluid Phase Equilib.* **216**, 201–217 (2004).
24. Coutinho, J. A. P. & Stenby, E. H. Predictive local composition models for solid/liquid equilibrium in n-alkane systems: Wilson equation for multicomponent systems. *Ind. Eng. Chem. Res.* **35**, 918–925 (1996).
25. Prausnitz, J. M. Thermodynamic and Transport Properties of Coal Liquids. *Fluid Phase Equilibria* vol. 35 316–318 (1987).
26. Li, H. & Zhang, J. A generalized model for predicting non-Newtonian viscosity of waxy crudes as a function of temperature and precipitated wax. *Fuel* **82**, 1387–1397 (2003).
27. Pauly, J., Daridon, J. L., Coutinho, J. A. P., Lindeloff, N. & Andersen, S. I. Prediction of solid-fluid phase diagrams of light gases-heavy paraffin systems up to 200 MPa using an equation of state-G(E) model. *Fluid Phase Equilib.* **167**, 145–159 (2000).
28. Ghanaei, E., Esmaeilzadeh, F. & Fathikalajahi, J. High pressure phase equilibrium of wax: A new thermodynamic model This paper is dedicated to the late Professor Jamshid Fathikalajahi. *Fuel* **117**, 900–909 (2014).
29. Ameri Mahabadian, M., Chapoy, A. & Tohidi, B. A New Thermodynamic Model for Paraffin Precipitation in Highly Asymmetric Systems at High Pressure Conditions. *Ind. Eng. Chem. Res.* **55**, 10208–10217 (2016).
30. Nasrifar, K. & Fani, M. Fluid Phase Equilibria Effect of pressure on the solid – liquid equilibria of synthetic paraffin mixtures using predictive methods. *Fluid Phase Equilib.* **310**, 111–119 (2011).

31. Simoncelli, A. P. P. *et al.* Phase behavior of systems with high CO2 content: Experiments and thermodynamic modeling. *Fluid Phase Equilib.* 112574 (2020) doi:10.1016/j.fluid.2020.112574.
32. Bamberger, A. & Maurer, G. High-pressure vapor-liquid equilibria in binary mixtures of carbon dioxide and aromatic hydrocarbons: Experimental data and correlation for CO2+ acetophenone, CO2+ 1-chloronaphthalene, CO2+ methyl benzoate and CO2+ n-propylbenzene. *J. Supercrit. Fluids* **7**, 115–127 (1994).
33. Awan, J. A., Tsivintzelis, I., Coquelet, C. & Kontogeorgis, G. M. Phase equilibria of three binary mixtures: Methanethiol + methane, methanethiol + nitrogen, and methanethiol + carbon dioxide. *J. Chem. Eng. Data* **57**, 896–901 (2012).
34. Sato, Y., Tagashira, Y., Maruyama, D., Takishima, S. & Masuoka, H. Solubility of carbon dioxide in eicosane, docosane, tetracosane, and octacosane at temperatures from 323 to 473 K and pressures up to 40 MPa. *Fluid Phase Equilib.* **147**, 181–193 (1998).
35. Pöhler, H., Scheidgen, A. L. & Schneider, G. M. Fluid phase equilibria of binary and ternary mixtures of supercritical carbon dioxide with a 1-alkanol and an n-alkane up to 100 MPa and 393 K - Cosolvency effect and miscibility windows (Part II). *Fluid Phase Equilib.* **115**, 165–177 (1996).
36. Hayduk, W., Walter, E. B. & Simpson, P. Solubility of Propane and Carbon Dioxide in Heptane, Dodecane, and Hexadecane. *J. Chem. Eng. Data* **17**, 59–61 (1972).
37. Gardeler, H., Fischer, K. & Gmehling, J. Experimental determination of vapor-liquid equilibrium data for asymmetric systems. *Ind. Eng. Chem. Res.* **41**, 1051–1056 (2002).
38. Aparicio-Martínez, S. & Hall, K. R. Phase equilibria in water containing binary systems from molecular based equations of state. *Fluid Phase Equilib.* **254**, 112–125 (2007).
39. Orr, F. M., Yu, A. D. & Lien, C. L. Phase Behavior of CO2 and Crude Oil in Low-Temperature Reservoirs. *Soc. Pet. Eng. J.* **21**, 480–492 (2007).
40. Huie, N. C., Luks, K. D. & Kohn, J. P. Phase-Equilibria Behavior of Systems Carbon Dioxide-n-Eicosane and Carbon Dioxide-n-Decane-n-Eicosane. *J. Chem. Eng. Data* **18**, 311–313 (1973).
41. Reverchon, E., Russo, P. & Stassi, A. Solubilities of Solid Octacosane and Triacontane in Supercritical Carbon Dioxide. *J. Chem. Eng. Data* **38**, 458–460 (1993).
42. García, J., Lugo, L. & Fernández, J. Phase equilibria, PVT behavior, and critical phenomena in carbon dioxide + n-alkane mixtures using the perturbed-chain statistical associating fluid theory approach. *Ind. Eng. Chem. Res.* **43**, 8345–8353 (2004).
43. Hosseinipour, A., Japper-Jaafar, A. B. & Yusup, S. The Effect of CO2 on Wax Appearance Temperature of Crude Oils. *Procedia Eng.* **148**, 1022–1029 (2016).
44. Pauly, J., Coutinho, J. & Daridon, J. L. High pressure phase equilibria in methane + waxy systems. 1. Methane + heptadecane. *Fluid Phase Equilib.* **255**, 193–199 (2007).

Phase Equilibria of Waxy Live Oil Systems containing CO_2: Experimental Measurements and Thermodynamic Modelling.

Oluwakemi V. Eniolorunda*, Antonin Chapoy, Rod Burgass.

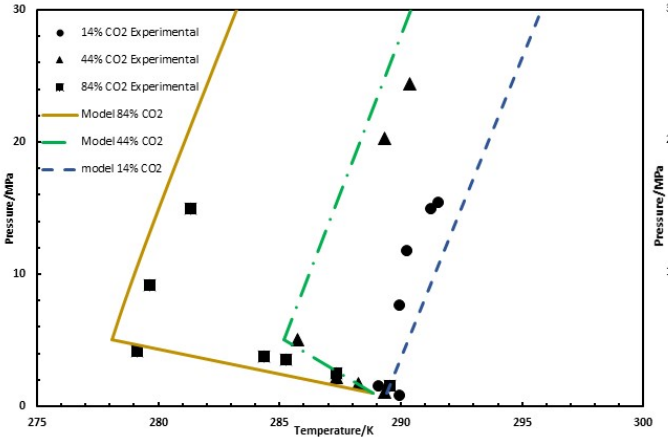

Fig.1 . Experimental data of 3 binary mixtures of CO_2 and n-C_{16}.

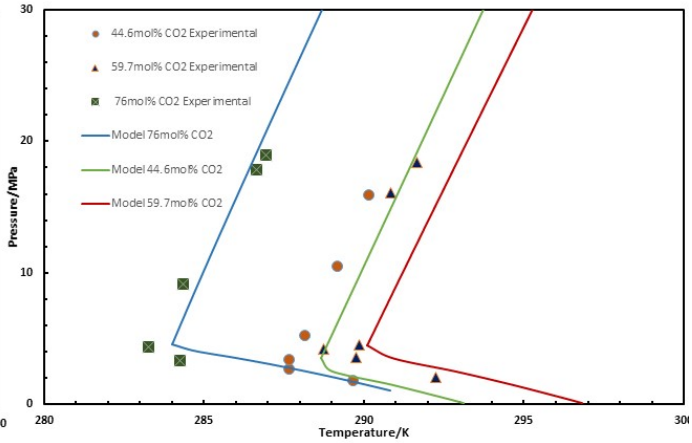

Fig. 2. Experimental solid-fluid phase boundary for multicomponent mixtures (Synthetic live oil) containing CO_2, n-C_{12}, n-C_{16}, n-C_{22}, n-C_{23} and n-C_{24}.